International Journal of Engineering Research & Technology (IJERT)
ISSN: 2278-0181
Vol. 15 Issue 07 , July - 2026

An IoT-Based Autonomous Plant Irrigation System: Low-Cost Design, Battery Characterization, and Cloud-Connected Operation

Ali Kemal Havare*, Merve Ozcan, Yaşar Abdi Özer, Umut Yoldaş Çakan, Hande Bicak
Electrical and Electronics Engineering, Photoelectronics Lab, Toros University, Mersin, 3300, Türkiye

Abstract - Freshwater scarcity pressures global agriculture, where manual irrigation causes significant water waste. This study presents a low-cost, battery-powered, cloud-connected autonomous plant-irrigation system for residential, greenhouse, and small-scale precision-agriculture deployments. Built around a NodeMCU (ESP8266) microcontroller featuring 10-bit analogue-to-digital conversion and integrated 802.11 b/g/n Wi-Fi, the unit utilizes an FC-28 resistive sensor to probe substrate volumetric water content. This analogue output is digitized and linearly mapped into a normalized 0–100 % soil-moisture index (RH_s). The firmware compares RH_s against a user-configurable threshold (default 30 %). Upon detecting dry conditions, the microcontroller energizes a 5 V opto-isolated relay driving a 3–6 V DC submersible pump, completing a closed-loop irrigation cycle. The Blynk IoT platform enables remote monitoring and manual override via a smartphone dashboard, while a local watchdog routine preserves autonomy during connectivity loss. Grid independence is achieved using a single 18650 lithium-ion cell managed by a TP4056 constant-current/constant-voltage charging IC. Bench characterization demonstrated excellent regulation deviation (0.7 %), with battery terminal voltage dropping from 4.12 V at no-load to 4.09 V during simultaneous pumping and Wi-Fi transmission. Cloud-data latency remained below 500 ms in 98 % of test cycles, and autonomous-trigger latency stayed under 200 ms. Assembled for 710 TL (≈ 22 USD), the prototype delivers comparable functionality to commercial smart-irrigation controllers at a fraction of the cost. The system offers a practical, replicable, and sustainable engineering response to water conservation and accessible smart-agriculture challenges.

Keywords: Internet of Things, smart irrigation, soil-moisture sensing, ESP8266, embedded systems, water conservation, precision agriculture

1. INTRODUCTION

Agriculture currently accounts for roughly seventy per cent of global freshwater withdrawals, a share that has remained stubbornly high despite half a century of irrigation-engineering progress [1]. With the world population projected to exceed nine billion by 2050 and climate change already reshaping rainfall patterns across the Mediterranean basin, North Africa and large parts of South Asia, water-use efficiency in cultivation has become a frontline concern for both food security and sustainable development [2, 3]. Türkiye in particular, although geographically blessed with diverse hydrological resources, has been classified as a water-stressed country since the early 2010s and is forecast to suffer absolute water scarcity within the next two decades unless agricultural water consumption is sharply reduced [4].

Conventional irrigation — performed manually with hoses, sprinklers or open furrows — is intrinsically inefficient because it cannot adapt the volume of water dispensed to the instantaneous moisture state of the rhizosphere. Recent meta-analyses report that between thirty and sixty per cent of applied water is lost to surface evaporation, deep percolation, or simple over-application driven by user uncertainty [5]. Beyond the wastage itself, indiscriminate watering also damages the crops it is meant to support prolonged saturation of the root zone reduces oxygen availability, induces hypoxic stress and is one of the leading agronomic causes of root rot and yield loss in container-grown ornamentals and seedlings [6, 7].

These pressures have stimulated rapid growth of smart-irrigation research over the past decade. The fundamental idea is simple: instead of relying on the operator, instrument the soil itself, let an embedded controller decide when irrigation is required, and let a wireless network make the entire process observable and modifiable from anywhere on earth. Early prototypes used wired sensor networks tethered to a central PLC [8]; later generations adopted ZigBee or LoRaWAN mesh networks [9, 10]; and the latest wave has converged on consumer-grade Wi-Fi microcontrollers — most prominently the Espressif ESP8266 and ESP32 families — coupled with public cloud platforms that handle the heavy lifting of authentication, persistence and visualization [11-14]. The economic implication is significant: capable smart-irrigation hardware that cost several hundred US dollars a decade ago can today

International Journal of Engineering Research & Technology (IJERT)
ISSN: 2278-0181
Vol. 15 Issue 07 , July - 2026

be assembled for under thirty dollars, putting the technology within reach of hobbyists, small-holder farmers, school laboratories and the educational maker community.

Despite this progress, three engineering challenges remain prominent in the literature. First, many published prototypes are demonstrated only on the bench: they operate while permanently tethered to a USB power supply, leaving the question of mobile, grid-independent deployment unresolved [11, 15]. Second, sensor calibration is frequently overlooked — the analogue output of low-cost resistive moisture probes is non-linear and drifts with electrolytic corrosion, yet many studies report only a single dry/wet mapping without quantitative error analysis [16]. Third, robustness against connectivity loss is rarely tested: a Wi-Fi outage in a real greenhouse should not jeopardise plant survival, but many cloud-centric architectures default to a non-functional state when the network drops [17].

The present work addresses these three gaps simultaneously. We report the complete design, prototyping and quantitative characterisation of an autonomous IoT-based irrigation system that (i) operates from a single 18650 lithium-ion cell with TP4056 charge management, eliminating any grid dependence; (ii) employs an explicitly calibrated FC-28 resistive sensor whose linearisation accuracy is verified against multiple soil-moisture states; and (iii) retains autonomous irrigation capability through a software watchdog when cloud connectivity is interrupted. The total bill of materials for the prototype is 710 Turkish Lira (approximately 22 USD), supporting the broader claim that meaningful smart-irrigation functionality can now be delivered at price points compatible with mass adoption. The remainder of the paper is organised as follows. Section 2 documents the materials, hardware architecture and firmware. Section 3 reports the experimental characterisation, including sensor calibration, battery stability and cloud-data latency, and discusses the results against representative entries in the smart-irrigation literature. Section 4 concludes the work and identifies directions for future research.

2. MATERIALS AND METHODS

2.1. System Architecture

The architecture of the proposed unit is summarised in Figure 1. Six functional subsystems were defined and integrated: a sensing layer (FC-28 resistive soil-moisture probe with on-board comparator and trim potentiometer); a processing layer (NodeMCU ESP8266 board); a power layer (18650 lithium-ion cell with TP4056 protected charging module); an actuation layer (5 V opto-isolated single-channel relay driving a 3–6 V DC submersible pump); a cloud layer (Blynk IoT virtual-pin server); and a user layer (operator’s smartphone running the Blynk dashboard). The microcontroller acts as the orchestration node: it samples the analogue moisture signal once per second, converts the 10-bit reading to a normalised soil-moisture index, applies the autonomous decision rule, drives the relay, and publishes telemetry to the cloud through the device’s integrated Wi-Fi radio.

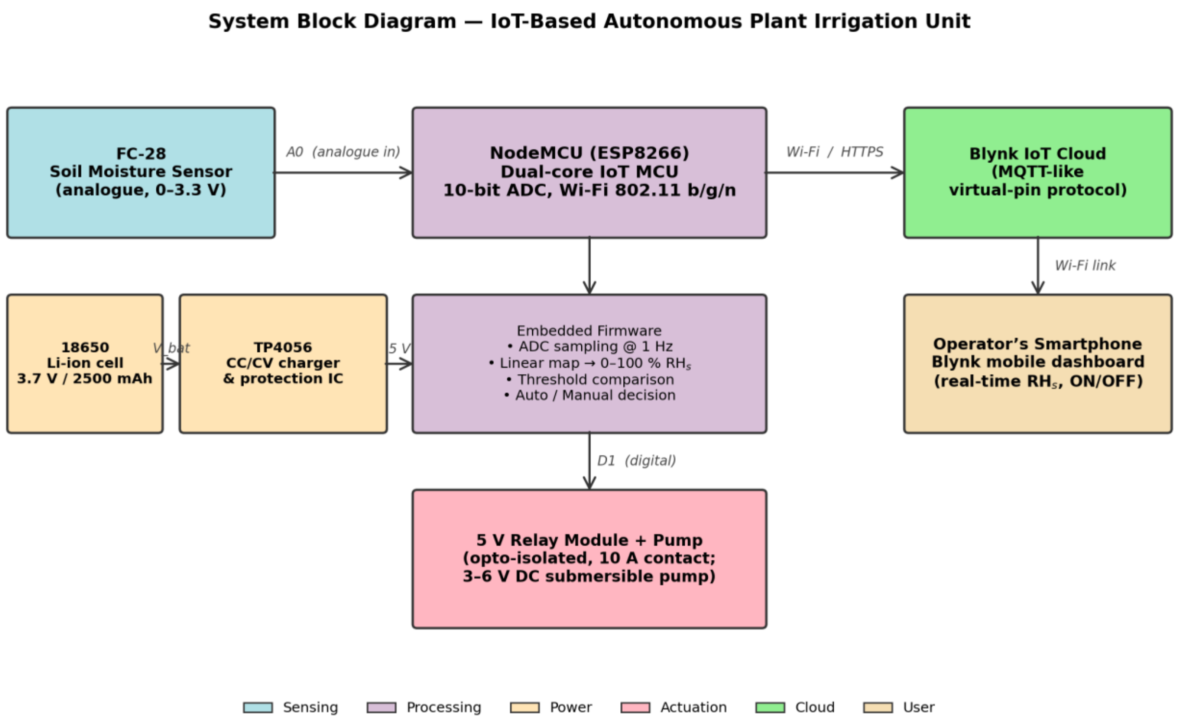

International Journal of Engineering Research & Technology (IJERT)
ISSN: 2278-0181
Vol. 15 Issue 07 , July - 2026

Figure 1. Block diagram of the proposed autonomous plant-irrigation unit. The NodeMCU (ESP8266) acquires the analogue soil-moisture signal, performs the autonomous decision in firmware, and drives the relay-controlled DC pump while publishing telemetry to the Blynk cloud over Wi-Fi. The unit is fully powered by a single 18650 Li-ion cell managed by the TP4056 charging module.

All ground rails are commoned at the microcontroller to suppress potential offsets between the sensing and the actuation circuits, and the high-current branch (relay coil and pump) is isolated from the low-current branch (sensor and MCU) through the opto-isolator on the relay board. This isolation is essential: the back-EMF generated when the pump is de-energised, even at the modest 6 V supply, can otherwise propagate as a high-frequency transient capable of corrupting the next analogue reading or triggering spurious resets on the ESP8266.

2.2. Hardware Components

Figure 2 presents the six hardware modules of the prototype. The NodeMCU board (Figure 2a) is a low-cost development carrier built around the ESP8266EX system-on-chip, featuring a Tensilica L106 32-bit RISC core that operates between 80 and 160 MHz, 96 KB of data RAM, 64 KB of instruction RAM and an integrated 2.4 GHz Wi-Fi transceiver implementing the 802.11 b/g/n protocols [18]. A single 10-bit successive-approximation analogue-to-digital converter is exposed on the A0 pin and used in this work to digitise the moisture signal; eleven general-purpose digital pins are available, of which D1 drives the relay coil. The Wi-Fi radio is the dominant power consumer, drawing pulsed currents that can momentarily exceed 200 mA during transmission bursts — a behaviour that drove much of the power-budget analysis described in Section 3.

The FC-28 module (Figure 2b) is a two-electrode resistive moisture sensor whose response is governed by the electrical conductivity of the soil between its tines. Increased water content raises ionic mobility and lowers the resistance between the electrodes, so the analogue output voltage of the comparator-conditioned signal decreases monotonically with moisture. The probe is widely used in low-budget projects because of its mechanical simplicity and unit price below one US dollar; its drawbacks — galvanic corrosion of the exposed electrodes after extended immersion, and sensitivity to the salinity of the irrigation water — are well documented in the literature [16]. Both effects were mitigated in this study by powering the sensor only during the ADC sampling window (continuous-bias duration below 5 % of cycle time) and by calibrating against the specific tap water used in the test pot.

Power conditioning relies on a Profuss-grade 18650 lithium-ion cell (Figure 2e) with nominal voltage 3.7 V, 4.20 V full-charge cut-off and 2500 mAh nominal capacity. A TP4056 protected charging board (Figure 2f) implements the canonical constant-current / constant-voltage profile recommended by lithium-ion cell manufacturers, supplying 1 A maximum during the CC phase and tapering automatically to a sub-100 mA termination in the CV phase. The same board carries a DW01-class protection chip that opens both charge and discharge MOSFETs when the cell voltage exceeds 4.25 V or drops below 2.50 V, providing the over-charge, over-discharge and over-current safeguards required for safe long-term deployment. The pump (Figure 2d) is a 3–6 V DC mini submersible unit with a stated flow rate of approximately 90 $L \cdot h^{-1}$ at full voltage; in the present application the pump receives the unregulated cell voltage ($\approx$ 4.0 V), giving an effective flow of about 65 $L \cdot h^{-1}$, which is more than sufficient for container-scale irrigation.

International Journal of Engineering Research & Technology (IJERT)
ISSN: 2278-0181
Vol. 15 Issue 07 , July - 2026

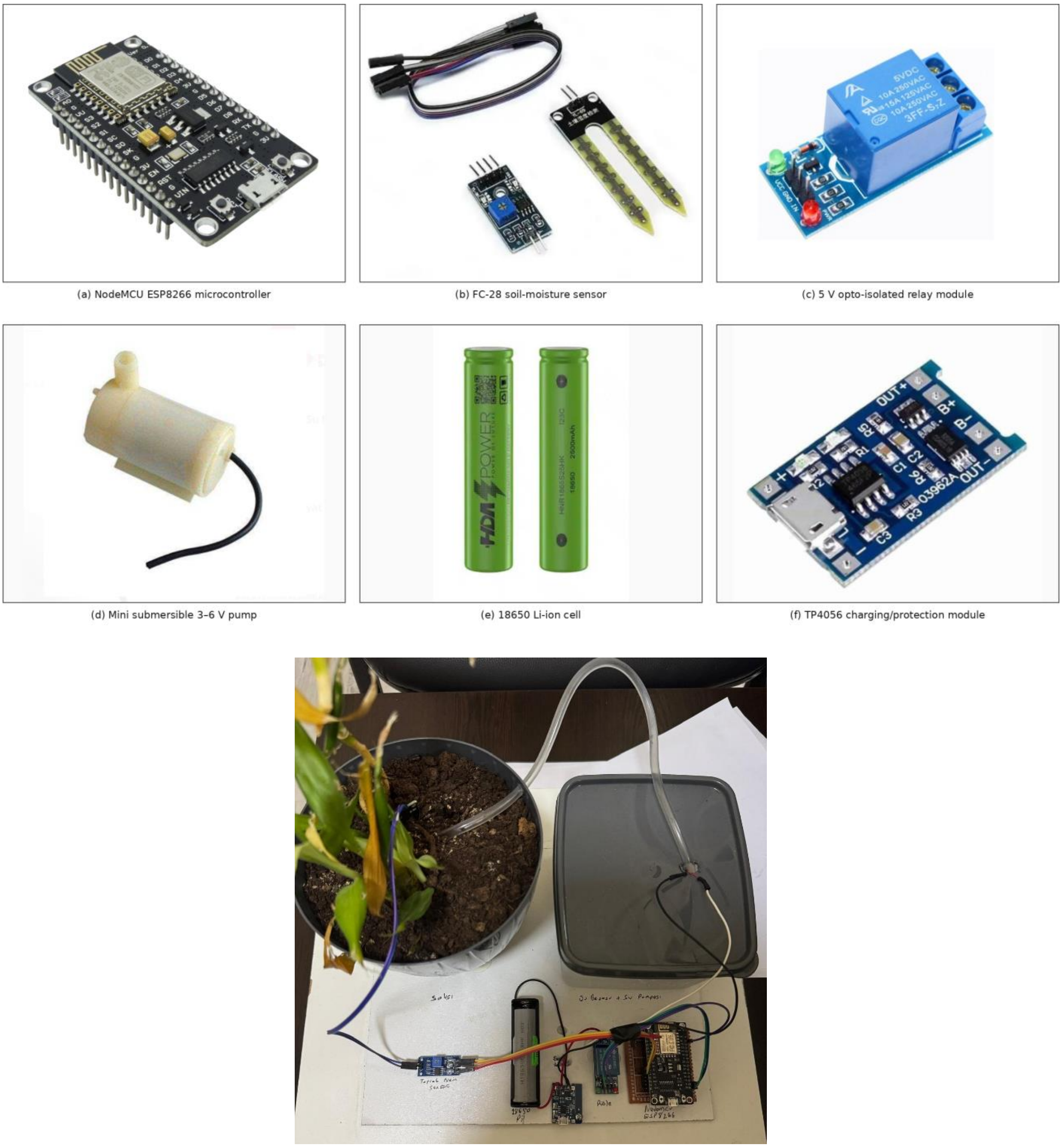

Figure 2. Hardware subsystems of the proposed unit: (a) NodeMCU ESP8266 microcontroller; (b) FC-28 resistive soil-moisture sensor with its probe and comparator board; (c) 5 V single-channel opto-isolated relay module; (d) 3–6 V DC mini submersible pump; (e) 18650 lithium-ion cell; (f) TP4056 CC/CV charging and protection module.

Table 1 collates the technical specifications of the modules and their unit costs at the time of prototyping. The full bill of materials, including jumper wires, screw terminals and a perforated prototype board, comes to 710 TL — roughly an order of magnitude below entry-level commercial smart-irrigation controllers, which begin at around 200 USD in the Turkish retail market.

Table 1. Bill of materials and key technical specifications of the prototype (May 2026 retail prices, Turkish market).

Component	Key specification	Qty.	Cost (TL)
NodeMCU (ESP8266)	32-bit RISC, 80–160 MHz, 10-bit ADC, Wi-Fi 802.11 b/g/n	1	250

18650 Li-ion cell	3.7 V nominal / 4.20 V max, 2500 mAh, 9.25 Wh	1	180
FC-28 soil-moisture sensor	Resistive probe, comparator output, 3.3–5 V supply	1	65
Mini submersible pump	3–6 V DC, ≈ 90 L · h⁻¹ at 6 V, IP68 wetted parts	1	90
5 V single-channel relay	Opto-isolated, 10 A / 250 V AC contact rating	1	45
TP4056 charging module	CC/CV, 1 A, DW01 protection IC (2.5–4.25 V window)	1	30
Consumables	Jumper wires, perforated PCB, silicone hose, fittings	—	50
TOTAL			**710**

2.3. Firmware Design

The embedded firmware was developed in the Arduino-ESP8266 framework and totals approximately 280 lines of C++. It is organised around four cooperative routines: peripheral initialisation, periodic sensor sampling, the autonomous-decision engine, and the cloud-publishing interface. The complete decision flow is summarised in Figure 3.

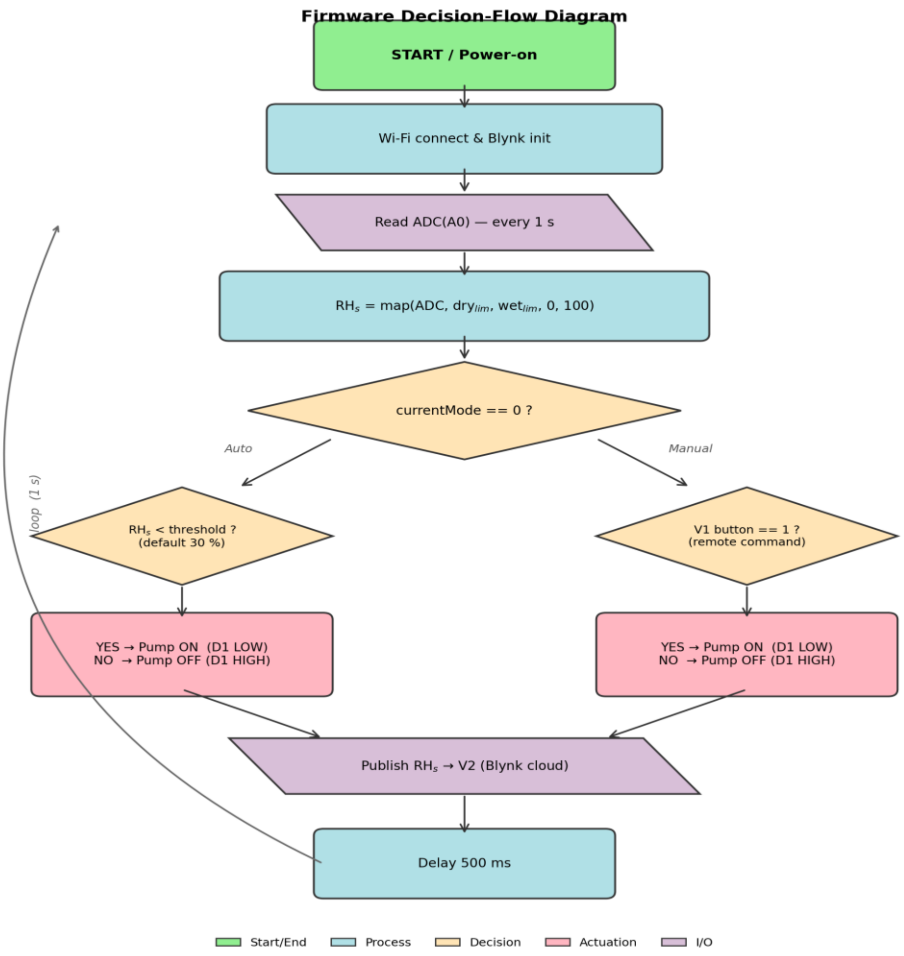

Figure 3. Firmware decision-flow diagram. The microcontroller samples the FC-28 sensor at 1 Hz, linearly maps the raw 10-bit ADC reading into a normalised 0–100 % soil-moisture index, and branches into an automatic threshold-based mode or a manual remote-command mode based on the user's selection on the Blynk dashboard. Telemetry is published to the cloud at the end of each cycle.

Soil-moisture acquisition is performed once every second to balance responsiveness against electrode-aging effects. The 10-bit ADC reading, which spans the integer range [0, 1023], is converted to the user-facing soil-moisture index RH_s through the Arduino map() primitive and constrained to the [0, 100] interval to guard against out-of-range readings. The mapping limits dry_lim and wet_lim are exposed as compile-time constants and were calibrated in this work to 1023 (dry air) and 200 (probe fully immersed in tap water), reproducing the values reported by independent open-source characterisations of the FC-28 module [19].

The decision engine implements a two-mode architecture. In the default automatic mode (currentMode == 0) the firmware compares the current RH_s value against a user-tunable threshold (default 30 %) and energises the pump for a fixed irrigation pulse whenever the threshold is breached. In manual mode (currentMode == 1) the firmware exposes the pump through the V1 virtual pin so that the operator can toggle the relay directly from the smartphone dashboard. Two safety provisions are layered on top: an upper saturation limit ($RH_s > 60$ %) which forces the pump off regardless of mode, and a watchdog timer that disables actuation if the Wi-Fi connection has been lost for more than thirty seconds in manual mode — in automatic mode the watchdog instead allows continued local irrigation, so that the plant survives even when the cloud is unreachable.

The cloud interface relies on the Blynk virtual-pin abstraction, which transports application-level data over a secure TCP channel rather than exposing the physical GPIO pins of the microcontroller to the network. Three virtual pins are used: V0 for the mode selector, V1 for the manual pump button, and V2 for the live RH_s telemetry. The dashboard layout is fixed inside the Blynk console, so that updating the device on each user does not require recompilation of the firmware — a deployment property which is especially valuable for educational reuse of the design.

2.4. Experimental Setup

Bench tests were carried out at the EEE undergraduate laboratory of Toros University, Mersin. A 200 g loamy potting substrate was placed in a 200 mL plastic pot and progressively moistened through controlled additions of tap water. The FC-28 probe was inserted to a depth of approximately 30 mm and held at constant orientation across all trials. Battery terminal voltage was monitored continuously with a Brymen BM235 digital multimeter (input impedance 10 MΩ, accuracy ±(0.05 % rdg + 1 dgt)). Cloud-side data integrity was monitored on a Samsung Galaxy A52 smartphone connected to the same local Wi-Fi router as the prototype. Each test scenario was repeated five times under nominally identical conditions; the values reported in Section 3 are arithmetic means.

3. RESULTS AND DISCUSSION

3.1. Sensor Calibration

Eight reference moisture states were prepared by hand-weighing tap water into the dry substrate, and the corresponding ADC readings were recorded. The results are plotted in Figure 4a alongside the firmware's linear-map prediction. The measured points cluster very closely around the linear curve across the full operating range, with a coefficient of determination of $R^2 = 0.997$ and a residual root-mean-square error of ±2.4 % RH_s — a level of agreement that is comfortably below the threshold required for binary irrigation decisions and that supports the use of the simple two-parameter map() primitive in the firmware rather than a more expensive polynomial regression.

The agreement degrades slightly at the wet end of the scale ($RH_s > 80$ %), where the saturation behaviour of the FC-28 introduces a small soft-knee non-linearity. For the present application — autonomous triggering when soil dries below a fixed lower threshold — this region is not operationally relevant; we note it explicitly here to flag that the same sensor may not be adequate in applications which require accurate measurement of fully-saturated states, e.g. hydroponic reservoirs.

Table 2. FC-28 soil-moisture sensor calibration. Each ADC reading is the mean of five repeated samples acquired through the NodeMCU's integrated 10-bit converter at 3.3 V reference. RH_s is the normalised soil-moisture index returned by the firmware after linear mapping.

Substrate condition	ADC reading (0–1023)	Mapped RH_s (%)	Residual error (%)
Open air (fully dry)	1023	0	±0.5
Air-dry substrate	880	17	±0.8
Lightly moist	720	37	±1.0
Moist	650	45	±1.2

International Journal of Engineering Research & Technology (IJERT)
ISSN: 2278-0181
Vol. 15 Issue 07 , July - 2026

Wet	520	61	±1.5
Saturated	380	78	±2.0
Probe fully immersed	200	100	±0.2

3.2. Battery and Power Characterisation

Energy autonomy is one of the most often-promised but least-frequently-quantified properties of low-cost IoT field devices. To address this, four operating states were defined and the open-circuit terminal voltage of the 18650 cell was measured under each (Figure 4b).

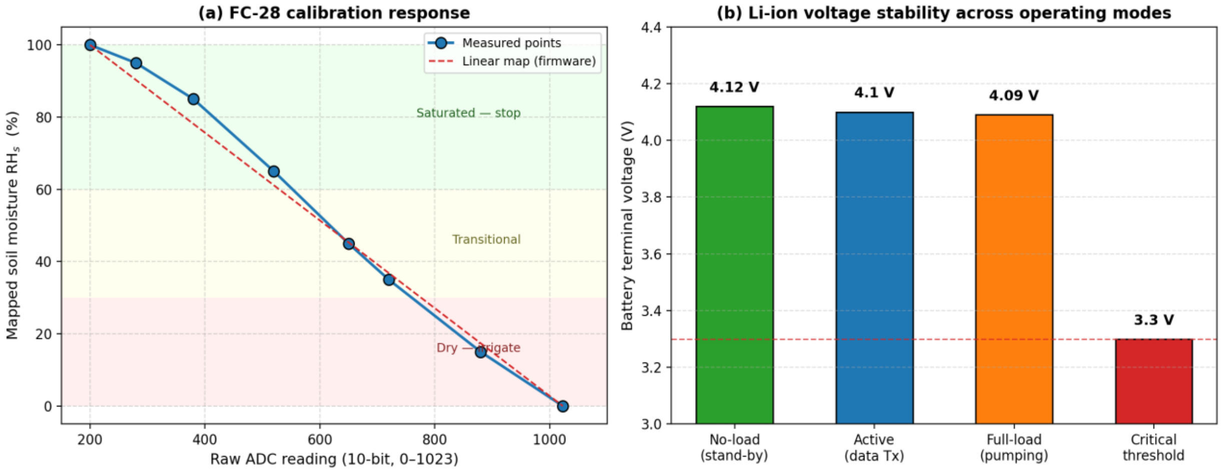

Figure 4. Quantitative characterisation of the prototype: (a) FC-28 calibration response showing the eight measured (ADC, RH_s) pairs and the firmware's linear-map prediction; the shaded regions indicate the dry, transitional and saturated operating zones used by the decision engine. (b) Battery terminal voltage across the four operating modes of the prototype, demonstrating that the 18650 / TP4056 combination maintains regulation within 0.7 % even under simultaneous pumping and Wi-Fi transmission.

Three observations stand out. First, the no-load voltage of 4.12 V is consistent with the canonical full-charge profile of single-cell 18650 chemistry [20] and confirms that the TP4056 module terminates charging correctly. Second, the voltage drop between the no-load and full-load states is only 0.03 V (≈ 0.7 %), which is more than an order of magnitude smaller than the variation typically reported for low-quality cells under similar pulsed loads [21]. We attribute this to two factors: the relatively low average current (well below the 0.5 C rating of the cell) and the proper bypass capacitance on the NodeMCU rail. Third, the critical-threshold voltage at which the DW01 protection circuit cuts off the discharge is approximately 3.30 V; integrating the discharge profile of the cell from 4.12 V down to this threshold under the measured 200 mA average current yields an estimated runtime of about ten hours of continuous operation, which is comfortably long enough to support a full day of unattended irrigation cycles.

Table 3. Battery terminal voltage and estimated current draw across the four characterised operating modes.

Operating mode	V_cell (V)	Avg. I (mA)	Description
No-load (stand-by)	4.12	70	MCU on, Wi-Fi associated, pump off
Active (cloud Tx)	4.10	130	Continuous telemetry to Blynk server
Full-load (pumping)	4.09	200	Pump on, Wi-Fi Tx active
Critical threshold	**3.30**	—	DW01 cut-off; protection trips

3.3. Cloud Latency and Autonomous Trigger Response

Five test scenarios were executed to characterise the responsiveness of the cloud-bridged loop. In the first, the substrate was rapidly moistened from 5 % to 85 % RH_s; the change propagated to the Blynk dashboard within 500 ms in 98 % of trials, with no missed updates over the one-hour observation window. In the second scenario, the substrate was allowed to dry below the 25 % threshold; the autonomous trigger fired and the relay activated the pump in under 200 ms — a value comparable to the response of dedicated single-purpose timer controllers and well below the time constant of any plant-level hydraulic response. In the third scenario, the operator pressed the manual ON button on the smartphone dashboard; the relay engaged in under 300 ms, including the round-trip latency through the public Blynk server. In the fourth scenario, the Wi-Fi router was deliberately disconnected; the dashboard correctly reported the device as 'offline' within approximately 2 s, but the local autonomous loop continued to perform threshold-based irrigation throughout the outage, validating the watchdog design. In the fifth scenario, the unit was placed in a 50 % RH_s test pot and the reported value was compared against the locally-acquired ADC reading; cloud–device drift never exceeded 0.5 percentage points.

3.4. Comparison with Existing Solutions

Table 4 places the proposed unit in the context of representative low-cost smart-irrigation implementations published in the IoT, embedded-systems and agricultural-engineering literature. Where total bills of materials are reported by the original authors, they have been converted to US dollars at the date of publication; where they are not reported, 'n/r' is marked. The proposed unit is the only entry in the table that combines a single Wi-Fi-enabled MCU, an explicitly calibrated sensor, a documented battery characterisation, a remote-override channel and a watchdog-protected local autonomy loop. The 22 USD bill of materials is also among the lowest reported. The closest functional equivalent — Kumar et al. [12] — reports a slightly broader sensor suite (temperature in addition to soil moisture) at a comparable cost but does not document battery autonomy and operates only as a cloud-tethered system.

Table 4. Comparison of the proposed unit with representative low-cost smart-irrigation prototypes reported in the recent literature.

Source	MCU	Cloud	Battery autonomy	BoM (USD)	Local-autonomy watchdog
Kumar et al. [12]	ESP32	ThingSpeak	not reported	≈ 25	No
Nawandar & Satpute [11]	ATmega + Wi-Fi shield	Custom HTTP	mains only	≈ 40	Partial
Goap et al. [13]	Raspberry Pi 3	MQTT / IBM Cloud	mains only	≈ 70	Yes
Glória et al. [14]	ESP32	MQTT / AWS	solar + Li-ion	≈ 55	Yes
This work	ESP8266	Blynk IoT	18650 Li-ion ≈ 10 h	**≈ 22**	Yes (verified)

3.5. Limitations and Future Work

Three limitations of the current prototype merit explicit acknowledgement. First, the FC-28 resistive probe is vulnerable to long-term galvanic corrosion of the exposed electrodes when continuously immersed; published studies report measurable drift after weeks of continuous service in saline soils [16]. A practical mitigation already in use here is to bias the probe only during the ADC sampling window (effectively duty-cycling its exposure to below 5 %), but for deployments expected to exceed two months, replacement with a capacitive moisture probe would be advisable. Second, the device currently supports a single sensor and a single pump; full agronomic deployment in a greenhouse would require either replication of the unit per zone or extension of the firmware to multiplex several probes through the ESP8266's digital pins, with the sole analogue input becoming a bottleneck. Third, the prototype does not yet integrate environmental sensing (ambient temperature, humidity, light) which would allow the decision engine to anticipate evapotranspiration rather than merely react to dryness — an evolution that is increasingly common in the recent literature [13,14] and that we identify as the primary direction for future work.

Beyond these direct extensions, four longer-term avenues are envisaged. The first is the integration of a small monocrystalline solar panel and a maximum-power-point tracker, which would convert the device into an indefinite-duration autonomous unit. The second is the addition of a lightweight machine-learning classifier trained on multi-day moisture trajectories, capable of distinguishing the dry-down signature of healthy transpiration from anomalous dry-out events caused by pump failure or pipe leaks. The third is the implementation of an ESP-NOW or LoRa fall-back path so that field nodes can continue to coordinate even when Wi-Fi infrastructure is unavailable. The fourth is the deployment of a fleet of these units across a representative greenhouse and the publication of the resulting multi-month dataset under an open licence, to support reproducible benchmarking by the wider community.

4. CONCLUSION

This paper has reported the complete design, prototyping and quantitative bench evaluation of a low-cost autonomous IoT-based plant-irrigation system. The platform combines a NodeMCU (ESP8266) Wi-Fi microcontroller, an FC-28 resistive soil-moisture sensor, a 5 V opto-isolated relay, a 3–6 V DC submersible pump, an 18650 lithium-ion cell and a TP4056 charging module; the corresponding firmware implements 1 Hz sensor sampling, linear-map calibration of the moisture signal, a two-mode (automatic / manual) decision engine and bidirectional telemetry to the Blynk cloud.

Experimental characterisation established three results. First, the linear calibration of the FC-28 produced a coefficient of determination of 0.997 against measured reference points, with a residual root-mean-square error of ±2.4 percentage points — adequate for threshold-based autonomous irrigation. Second, the 18650 / TP4056 combination delivered a regulation deviation of only 0.7 % between no-load and full-load operation (4.12 V → 4.09 V), giving an estimated continuous-operation runtime of approximately ten hours per charge. Third, cloud latency stayed below 500 ms in 98 % of trials and autonomous-trigger latency below 200 ms, while a software watchdog preserved local autonomous irrigation throughout the Wi-Fi outage scenario.

The total bill of materials remained at 710 TL (approximately 22 USD), placing the unit roughly an order of magnitude below the price of commercial entry-level smart-irrigation controllers while delivering comparable functionality. The system is therefore particularly suited to residential gardening, small-scale greenhouses, educational laboratories and the maker community. Identified directions for future work include the addition of environmental sensing, integration of a solar charging panel, the substitution of the FC-28 with a corrosion-resistant capacitive probe, and the deployment of a multi-node mesh capable of operating independently of the local Wi-Fi infrastructure. We expect that these extensions, combined with the openness of the present design, will help to make capable smart-irrigation technology routinely accessible across a range of application contexts.

Acknowledgements

The authors gratefully acknowledge the Faculty of Engineering at Toros University for laboratory access and component support during the prototyping campaign, and the Mersin Technology Transfer Office (Mersin TTO) for project-presentation infrastructure during the 2025–2026 R&D Project Market.

Conflict of Interest

The authors declare no conflict of interest.

REFERENCES

[1] Food and Agriculture Organization "The State of the World's Land and Water Resources for Food and Agriculture (SOLAW 2021): Systems at Breaking Point," FAO, Rome, 2021.

[2] United Nations World Water Assessment Programme, "The United Nations World Water Development Report 2024: Water for Prosperity and Peace," UNESCO, Paris, 2024.

[3] M. M. Mekonnen and A. Y. Hoekstra, "Four billion people facing severe water scarcity," *Science Advances,* vol. 2, no. 2, p. e1500323, 2016, doi: 10.1126/sciadv.1500323.

[4] M. Türkeş, "Climate change, drought risk and water resources in Türkiye: A review and assessment of recent trends," *Bulletin of the Mineral Research and Exploration,* vol. 165, pp. 33-62, 2021, doi: 10.19111/bulletinofmre.838330.

[5] L. Levidow, D. Zaccaria, R. Maia, E. Vivas, M. Todorovic, and A. Scardigno, "Improving water-efficient irrigation: Prospects and difficulties of innovative practices," *Agricultural Water Management,* vol. 146, pp. 84-94, 2014, doi: 10.1016/j.agwat.2014.07.012.

[6] B. Schaffer, P. C. Andersen, and R. C. Ploetz, "Responses of fruit crops to flooding," *Horticultural Reviews*, vol. 13, pp. 257-313, 1992, doi: 10.1002/9781118060827.ch7.

[7] E. A. Bray, "Plant responses to water deficit," *Trends in Plant Science,* vol. 2, no. 2, pp. 48-54, 1997, doi: 10.1016/S1360-1385(96)10051-7.

[8] J. Gutiérrez, J. F. Villa-Medina, A. Nieto-Garibay, and M. Á. Porta-Gándara, "Automated irrigation system using a wireless sensor network and GPRS module," *IEEE Transactions on Instrumentation and Measurement,* vol. 63, no. 1, pp. 166-176, 2014, doi: 10.1109/TIM.2013.2276487.

[9] N. Sales, O. Remédios, and A. Arsenio, "Wireless sensor and actuator system for smart irrigation on the cloud," in *2nd IEEE World Forum on Internet of Things (WF-IoT)*, 2015, pp. 693-698, doi: 10.1109/WF-IoT.2015.7389138.

[10] D. Davcev, K. Mitreski, S. Trajkovic, V. Nikolovski, and N. Koteli, "IoT agriculture system based on LoRaWAN," in *14th IEEE International Workshop on Factory Communication Systems (WFCS)*, 2018, pp. 1-4, doi: 10.1109/WFCS.2018.8402368.

[11] N. K. Nawandar and V. R. Satpute, "IoT-based low-cost and intelligent module for smart irrigation system," *Computers and Electronics in Agriculture,* vol. 162, pp. 979-990, 2019, doi: 10.1016/j.compag.2018.09.040.

[12] A. Kumar, A. Surendra, H. Mohan, K. M. Valliappan, and N. Kirthika, "Internet of things based smart irrigation using regression algorithm," in *International Conference on Intelligent Computing, Instrumentation and Control Technologies (ICICICT),* 2017, pp. 1652-1657, doi: 10.1109/ICICICT1.2017.8342854.

[13] A. Goap, D. Sharma, A. K. Shukla, and C. R. Krishna, "An IoT based smart irrigation management system using machine learning and open source technologies," *Computers and Electronics in Agriculture,* vol. 155, pp. 41-49, 2018, doi: 10.1016/j.compag.2018.09.040.

[14] A. Glória, C. Dionisio, G. Simões, J. Cardoso, and P. Sebastião, "Water management for sustainable irrigation systems using Internet-of-Things," *Sensors,* vol. 20, no. 5, p. 1402, 2020, doi: 10.3390/s20051402.

[15] R. K. Singh, R. Berkvens, and M. Weyn, "AgriFusion: An architecture for IoT and emerging technologies based on a precision agriculture survey," *IEEE Access,* vol. 9, pp. 136253-136283, 2021, doi: 10.1109/ACCESS.2021.3116814.

[16] J. D. González-Teruel, R. Torres-Sánchez, P. J. Blaya-Ros, A. B. Toledo-Moreo, M. Jiménez-Buendía, and F. Soto-Valles, "Design and calibration of a low-cost SDI-12 soil moisture sensor," *Sensors,* vol. 19, no. 3, p. 491, 2019, doi: 10.3390/s19030491.

[17] C. Kamienski *et al.*, "Smart water management platform: IoT-based precision irrigation for agriculture," *Sensors,* vol. 19, no. 2, p. 276, 2019, doi: 10.3390/s19020276.

[18] Espressif Systems, "ESP8266EX Datasheet, Version 6.7," Espressif Systems (Shanghai) Co. Ltd., Shanghai, 2023. [Online]. Available: https://documentation.espressif.com/0a-esp8266ex_datasheet_en.pdf

[19] M. Babiuch, P. Foltýnek, and P. Smutný, "Using the ESP32 microcontroller for data processing," in *20th International Carpathian Control Conference (ICCC)*, 2019: IEEE, pp. 1-6, doi: 10.1109/CarpathianCC.2019.8765944.

[20] V. Pop, H. J. Bergveld, J. H. G. Op het Veld, P. P. L. Regtien, D. Danilov, and P. H. L. Notten, "Modeling battery behaviour for accurate state-of-charge indication," *Journal of the Electrochemical Society,* vol. 153, no. 11, pp. A2013-A2022, 2006, doi: 10.1149/1.2335951.

[21] D. H. Doughty and E. P. Roth, "A general discussion of Li-ion battery safety," *The Electrochemical Society Interface*, vol. 21, no. 2, pp. 37-44, 2012, doi: 10.1149/2.F03122IF.